



## Short communication

Hierarchical porous  $\text{Li}_4\text{Mn}_5\text{O}_{12}$  nano/micro structure as superior cathode materials for Li-ion batteries

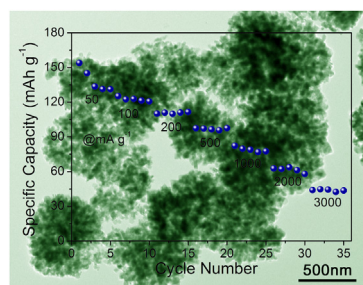
Yao Fu, Hao Jiang\*, Yanjie Hu, Ling Zhang, Chunzhong Li\*

Key Laboratory for Ultrafine Materials of Ministry of Education, School of Materials Science and Engineering, East China University of Science and Technology, Shanghai 200237, China

## HIGHLIGHTS

- Hierarchical porous  $\text{Li}_4\text{Mn}_5\text{O}_{12}$  nano/micro structure has been synthesized.
- The unique structure has the advantages of both nanostructure and microstructure.
- The  $\text{Li}_4\text{Mn}_5\text{O}_{12}$  cathode exhibits excellent electrochemical performances for LIBs.

## GRAPHICAL ABSTRACT



## ARTICLE INFO

## Article history:

Received 29 December 2013

Received in revised form

19 February 2014

Accepted 4 March 2014

Available online 13 March 2014

## Keywords:

 $\text{Li}_4\text{Mn}_5\text{O}_{12}$ 

Hierarchical porous nano/micro structure

Li-ion batteries

Cathode materials

## ABSTRACT

To overcome the disproportionation reaction and Jahn-Teller distortion of  $\text{Mn}^{3+}$  in  $\text{LiMn}_2\text{O}_4$  cathode materials, we demonstrate a facile route to synthesize hierarchical porous  $\text{Li}_4\text{Mn}_5\text{O}_{12}$  nano/micro structure, which consists of numerous well-crystallized nanoparticles with diameters of 20–30 nm. The unique structure combines the advantages of both nanostructure and microstructure. When applied as cathode materials for Li-ion batteries, it exhibited a very high specific capacity of 161  $\text{mAh g}^{-1}$  (theoretical value: 163  $\text{mAh g}^{-1}$ ) with intriguing rate performance and cycling stability.

© 2014 Elsevier B.V. All rights reserved.

## 1. Introduction

Lithium manganese oxides (LMO) have been widely studied as cathode materials for lithium ion batteries (LIBs) due to their intrinsic low-cost, environmental friendliness, abundant resources, and high safety [1–3]. Among this family, stoichiometric spinel  $\text{LiMn}_2\text{O}_4$  has gained the most extensive investigations [4,5]. However, the  $\text{LiMn}_2\text{O}_4$  suffers from large capacity fading during cycling due to the generation of soluble  $\text{Mn}^{2+}$  via a disproportionation

reaction ( $\text{Mn}^{3+} \rightarrow \text{Mn}^{2+} + \text{Mn}^{4+}$ ) at a high electrode potential, as well as Jahn-Teller distortion of  $\text{Mn}^{3+}$  ions [5,6]. To overcome these limitations, one effective way is to diminish the  $\text{Mn}^{3+}$  content in LMO, such as form  $\text{Li}_4\text{Mn}_5\text{O}_{12}$  where all the manganese ions are in the  $\text{Mn}^{4+}$  valence state. Actually, the spinel  $\text{Li}_4\text{Mn}_5\text{O}_{12}$  is also a promising cathode material for LIBs in view of its three-dimensional interstitial space for  $\text{Li}^+$  transport and high theoretical capacity of 163  $\text{mAh g}^{-1}$  [7–9]. For example, Zhao et al. [8] reported  $\text{Li}_4\text{Mn}_5\text{O}_{12}$  nanocrystallites prepared by spray-drying-assisted solid state reactions. Tian et al. [9] realized the synthesis of single crystalline  $\text{Li}_4\text{Mn}_5\text{O}_{12}$  nanowires by a molten salt route. However, there are very limited reports on  $\text{Li}_4\text{Mn}_5\text{O}_{12}$  in the

\* Corresponding authors. Tel.: +86 21 64250949; fax: +86 21 64250624.

E-mail addresses: [jianghao@ecust.edu.cn](mailto:jianghao@ecust.edu.cn) (H. Jiang), [czli@ecust.edu.cn](mailto:czli@ecust.edu.cn) (C. Li).

literature because of the difficulties in preparation resulting from the high covalent values of manganese atoms [8–10]. Besides, their electrochemical performances are still unsatisfactory.

Recently, much effort has been triggered to prepare nano/micro structured electrode materials for further improving the electrochemical performance [11–13]. In this regard, the nanosized primary particles can shorten the diffusion paths of  $\text{Li}^+$ , resulting in high rate performance. In addition, the microsized secondary structures can ensure a long-term cycle life and the endowment of a high volumetric energy density. For instance, Zhang et al. [14] reported a porous  $\text{Li}_4\text{Ti}_5\text{O}_{12}$  microspheres aggregated by nanosized particles. Li et al. [15] realized the synthesis of  $\text{LiNi}_{1/3}\text{Co}_{1/3}\text{Mn}_{1/3}\text{O}_2$  hollow nano/micro hierarchical microspheres. Both the resulting materials exhibited enhanced electrochemical performance as electrodes for LIBs. Unfortunately, hierarchical  $\text{Li}_4\text{Mn}_5\text{O}_{12}$  nano/micro structure still has not been realized until now.

Herein, we demonstrate a simple route to synthesize hierarchical porous  $\text{Li}_4\text{Mn}_5\text{O}_{12}$  nano/micro structure by using  $\text{MnO}_2$  ultrathin nanoflakes assembled microspheres as self-templates. The resulting unique structure consists of amounts of well-crystallized nanoparticles with diameters of  $\sim 20$ – $30$  nm. We believe it possesses three obvious advantages at least when applied as cathodes for LIBs. (a) The nanosized particles with high purity and crystallinity will greatly improve the utilization of active materials, and hence leading to a high specific capacity. (b) The porous feature can guarantee enough interaction between electrolyte and active materials, reducing  $\text{Li}^+$  diffusion paths. Meanwhile, the numerous pores are also expected to digest the possible volume expansion during the repeated  $\text{Li}^+$  insertion–extraction. (c) The microsized secondary structures will provide higher volumetric energy density than monodisperse nanoparticles. More importantly, we found that the as-synthesized  $\text{Li}_4\text{Mn}_5\text{O}_{12}$  cathodes exhibited a very high specific capacity with intriguing rate and cycling performances for LIBs.

## 2. Experimental section

### 2.1. Synthesis

All the reagents used in the experiments were of analytical grade (purchased from Sigma–Aldrich) and used without further purification. Firstly, ultrathin  $\text{MnO}_2$  nanoflakes aggregations were prepared by a simple strategy based on our previous report [15]. In a typical procedure, 0.396 g of  $\text{Mn}(\text{NO}_3)_2 \cdot 6\text{H}_2\text{O}$  and 0.1 g of triblock copolymer PEO-PPO-PEO (P123) were dissolved in 20 mL of deionized water. Then, 20 mL of 0.1 M  $\text{KMnO}_4$  as an aqueous solution was added dropwise into the above mixture at room temperature. After stirring for 10 min, the black precipitate was collected by filtration, washed with deionized water and absolute ethanol, and finally dried at  $60^\circ\text{C}$  for 6 h. The resulting products (ultrathin  $\text{MnO}_2$  nanoflakes assembled microsphere) were dissolved into hexane, and then mixed with  $\text{LiOH} \cdot \text{H}_2\text{O}$  dispersed in ethanol with a stoichiometric ratio ( $\text{Li}/\text{Mn} = 1:1.25$ ), following by stirring at  $60^\circ\text{C}$  until dried. Finally, hierarchical porous  $\text{Li}_4\text{Mn}_5\text{O}_{12}$  nano/micro structure was obtained after the above mixture was annealed at  $600^\circ\text{C}$  for 6 h in air.

### 2.2. Characterization

The as-prepared products were characterized with X-ray powder diffractometer (XRD; Rigaku D/Max 2550,  $\text{Cu K}\alpha$  radiation) at a scan rate of  $1^\circ \text{ min}^{-1}$ , scanning electron microscopy (FESEM; Hitachi, S-4800), and transmission electron microscopy (TEM; JEOL, JEM-2100F) operated at 200 kV.

### 2.3. Electrochemical measurements

Electrochemical measurements were performed using coin-type 2016 cells. The working electrode were prepared by mixing the as-synthesized active materials, carbon black, and poly(vinyl difluoride) (PVDF) with a weight ratio of 70:20:10, and then pasted on pure Al foil. The electrode area was  $1.13 \text{ cm}^2$ . The active materials loading was about  $0.4 \text{ mg cm}^{-2}$  with a thickness of  $50 \mu\text{m}$ . Pure lithium foil was used as counter electrode, and the separator was a polypropylene membrane (Celgard 2400). The electrolyte consists of a solution of 1 M  $\text{LiPF}_6$  in ethylene carbonate (EC)/dimethyl carbonate (DMC) (1:1 in volume). The cells were assembled in an argon-filled glove box. Cyclic voltammogram experiment was performed on an Autolab PGSTAT302N electrochemical workstation at scan rates of  $0.1 \text{ mV s}^{-1}$ . The charge and discharge measurements were carried out on a LAND-CT2001C test system at different current densities.

## 3. Results and discussion

Fig. 1 shows the XRD pattern of the hierarchical porous  $\text{Li}_4\text{Mn}_5\text{O}_{12}$  nano/micro structure. All of the diffraction peaks can be readily indexed to  $\text{Li}_4\text{Mn}_5\text{O}_{12}$  with spinel phase of face-centered cubic structure (JCPDS, No: 46-0810). No other characteristic peaks from impurities, such as  $\text{LiMn}_2\text{O}_4$ ,  $\text{MnO}_2$ , are detected in the pattern, indicating a high purity. And the strong diffraction peaks in the pattern also suggest a highly crystalline nature of the as-synthesized  $\text{Li}_4\text{Mn}_5\text{O}_{12}$ .

The corresponding SEM image was shown in Fig. 2, which revealed that the spherical aggregations are made of many nanoparticles. Detailed structural information was further investigated by TEM observations. From a low magnification TEM image (Fig. 3a), amounts of pores are clearly observed in each spherical aggregation. Fig. 3b shows a representative hierarchical porous  $\text{Li}_4\text{Mn}_5\text{O}_{12}$  nano/micro structure assembled from numerous nanoparticles with diameters of  $\sim 20$ – $30$  nm, which is in agreement with the SEM result. It is worth mentioning that such a hierarchical porous nano/micro structure is robust and it cannot be destroyed into fragments or primary nanoparticles even under severe ultrasonic treatment. The high resolution TEM images further reveal the stability of the spherical aggregations. In Fig. 3c, it can be observed that a crystal boundary (the area in the yellow box) exists between the adjacent  $\text{Li}_4\text{Mn}_5\text{O}_{12}$  nanocrystallites. An interplanar spacing of  $0.47 \text{ nm}$  matches well with the distance of the (111) plane of  $\text{Li}_4\text{Mn}_5\text{O}_{12}$ . In another high resolution TEM image (Fig. 3d), the

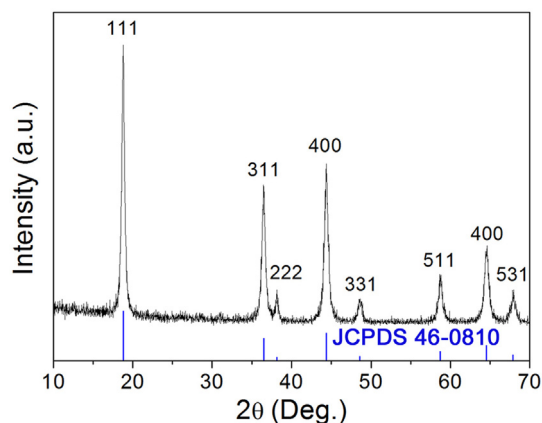
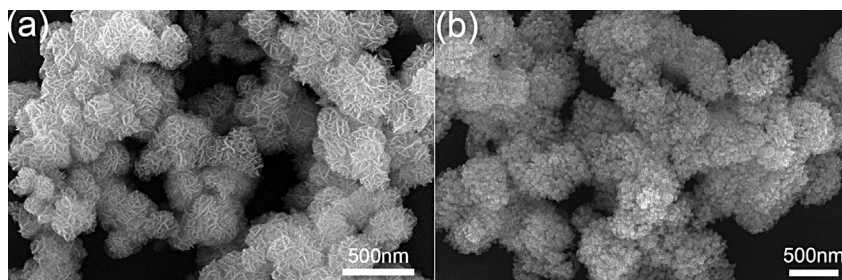


Fig. 1. XRD pattern of the as-prepared hierarchical porous  $\text{Li}_4\text{Mn}_5\text{O}_{12}$  nano/micro structure.



**Fig. 2.** SEM images of (a) the as-synthesized  $\text{MnO}_2$  ultrathin nanoflakes assembled microspheres and (b) the hierarchical porous  $\text{Li}_4\text{Mn}_5\text{O}_{12}$  nano/micro structure.

attached crystals are perfectly aligned at the contact areas between the adjacent particles. The SAED pattern (inset in Fig. 3d), which was detected from a typical spherical aggregation, indicates a polycrystalline nature. Unlike the simple physical contact, such kind of connection between adjacent nanocrystallites in the spherical aggregations can not only improve the structural integrity, but also effectively reduce the contact resistance among nanoparticles, which are beneficial for the enhancement of the rate performance and cycling stability.

To investigate the oxidation state of Mn, the sample was further characterized by XPS. Fig. 4a depicts the XPS spectrum of Mn 2p, where two peaks centered at 642.9 eV and 654.5 eV can be assigned to Mn 2p<sub>2/3</sub> and Mn 2p<sub>1/2</sub> binding energies, respectively, indicating Mn(IV) state in our sample [9]. The band at 530.0 eV (Fig. 4b) is attributed to the O 1s binding energy of the crystal lattice oxygen. [16] In addition, the molar ratio of O to Mn is calculated to be  $\sim 2.37$

based on the peak areas of their respective binding energy, which is nearly close to the theoretical value (2.40) of the  $\text{Li}_4\text{Mn}_5\text{O}_{12}$ .

The electrochemical performance of the hierarchical porous  $\text{Li}_4\text{Mn}_5\text{O}_{12}$  nano/micro structure as cathode materials for LIBs was evaluated. The cyclic voltammetry (CV) curves of the hierarchical porous  $\text{Li}_4\text{Mn}_5\text{O}_{12}$  nano/micro structure for the first five cycles at a scan rate of  $0.1 \text{ mV s}^{-1}$  in the voltage range 2–3.5 V (vs.  $\text{Li}^+/\text{Li}$ ) are shown in Fig. 5a. A couple of reversible redox peaks can be seen at 2.7/3.1 V, respectively, and from the second cycle onwards, the redox peaks overlapped substantially, indicating outstanding reversibility in the electrochemical process. Fig. 5b shows the charge/discharge curves of the as-prepared hierarchical porous  $\text{Li}_4\text{Mn}_5\text{O}_{12}$  nano/micro structure measured at a current density of  $50 \text{ mA g}^{-1}$  in a potential window of 2–3.5 V at room temperature. The voltage profiles present two obvious long plateaus at 2.8/2.95 V, exhibiting the typical characteristics of  $\text{Li}_4\text{Mn}_5\text{O}_{12}$  [9]. The

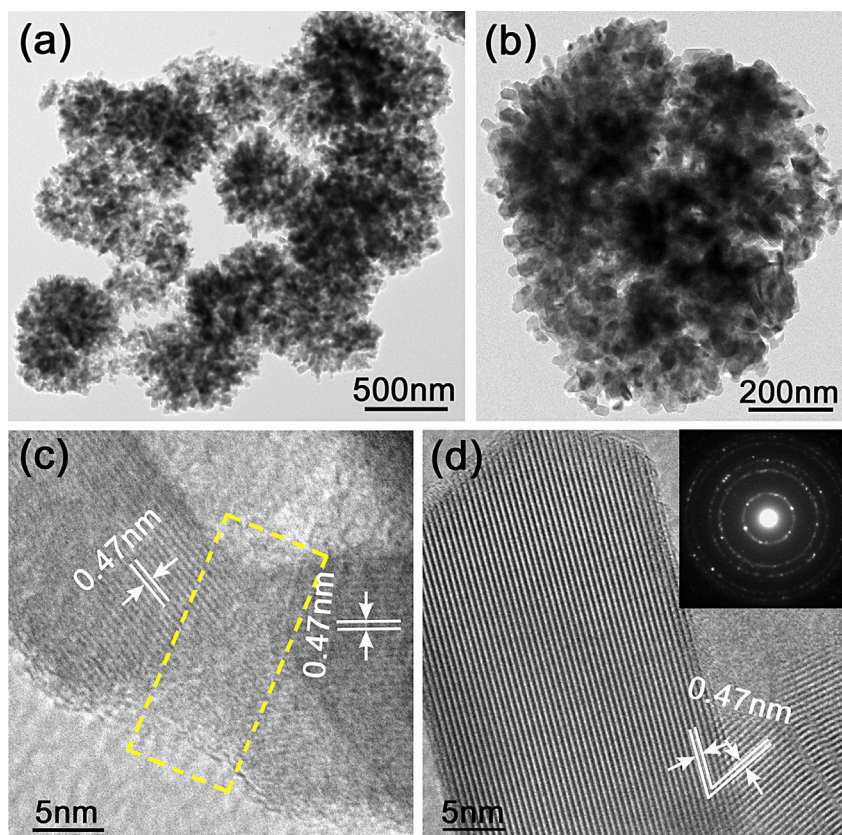


**Fig. 3.** (a) Low-, (b) high-magnification, (c) and (d) high resolution TEM images of the as-prepared hierarchical porous  $\text{Li}_4\text{Mn}_5\text{O}_{12}$  nano/micro structure (inset showing the SAED pattern).

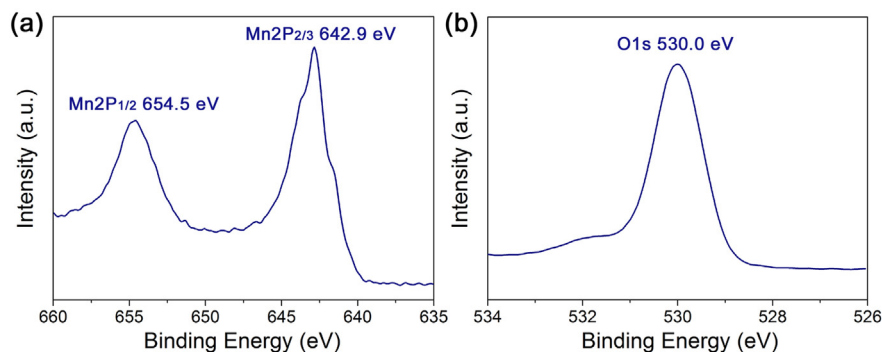


Fig. 4. (a) Mn 2p and (b) O 1s XPS spectra of the as-prepared hierarchical porous  $\text{Li}_4\text{Mn}_5\text{O}_{12}$  nano/micro structure.

discharge specific capacity can reach as high as  $161 \text{ mAh g}^{-1}$  (very close to the theoretical capacity of  $163 \text{ mAh g}^{-1}$ ). The special high specific capacity of our sample is mainly ascribed to the high utilization of active materials from the primary nanosized particles. In addition, the hierarchical porous feature enables rapid electrolyte transportation and active site accessibility. To the best of our knowledge, this is the highest specific capacity reported so far for the  $\text{Li}_4\text{Mn}_5\text{O}_{12}$  as LIBs cathodes. To further evaluate the rate performance, the hierarchical porous  $\text{Li}_4\text{Mn}_5\text{O}_{12}$  nano/micro structure was charged at  $50 \text{ mA g}^{-1}$  and then discharged at various current densities from 50 to  $3000 \text{ mA g}^{-1}$  within a potential window of 2–3.5 V, as shown in Fig. 5c. It can be observed that the discharge capacity of our sample slightly decreases to 122, 111, 97, 78, 62, and  $44 \text{ mAh g}^{-1}$  when the current rate increases to 100, 200, 500, 1000, 2000, and  $3000 \text{ mA g}^{-1}$ , respectively, demonstrating a high rate performance. The intriguing electrochemical performance, as predicted, is superior to the reported other  $\text{Li}_4\text{Mn}_5\text{O}_{12}$  structures in the literature, such as well-crystallized  $\text{Li}_4\text{Mn}_5\text{O}_{12}$  powder with grain size of 100–400 nm ( $135 \text{ mAh g}^{-1}$ ), [17] high-crystalline spinel  $\text{Li}_4\text{Mn}_5\text{O}_{12}$  nanowires ( $154 \text{ mAh g}^{-1}$ , but showing poor rate

performance) [9], and so forth. Recently, Zhao et al. [8] reported well-dispersed nanosized  $\text{Li}_4\text{Mn}_5\text{O}_{12}$  particles ( $<50 \text{ nm}$ ) with a specific capacity of  $158.7 \text{ mAh g}^{-1}$ , which was the highest value so far for  $\text{Li}_4\text{Mn}_5\text{O}_{12}$  cathode materials. However, the rate performance was not investigated. Such high electrochemical performance of our sample is mainly due to the unique configuration, in which the adjacent nanoparticles are well-contacted, improving the electrical conductivity. Meanwhile, it can also retain the structural integrity, leading to a high cycling stability.

The cycling behavior of the hierarchical porous  $\text{Li}_4\text{Mn}_5\text{O}_{12}$  nano/micro structure is shown in Fig. 5d, which was obtained at a current density of  $100 \text{ mA g}^{-1}$ . The discharge capacity gradually decreases but still maintains a high specific capacity of  $\sim 89 \text{ mAh g}^{-1}$  after 100 cycles. The corresponding TEM image is also provided in inset in Fig. 5d. There is no obvious morphology change on the hierarchical porous  $\text{Li}_4\text{Mn}_5\text{O}_{12}$  nano/micro structure even after 100 cycles. Notably, the Coulombic efficiency stays at nearly 100% in the overall battery operation. These results indicated that the hierarchical porous  $\text{Li}_4\text{Mn}_5\text{O}_{12}$  nano/micro structure had good electrochemical stability.

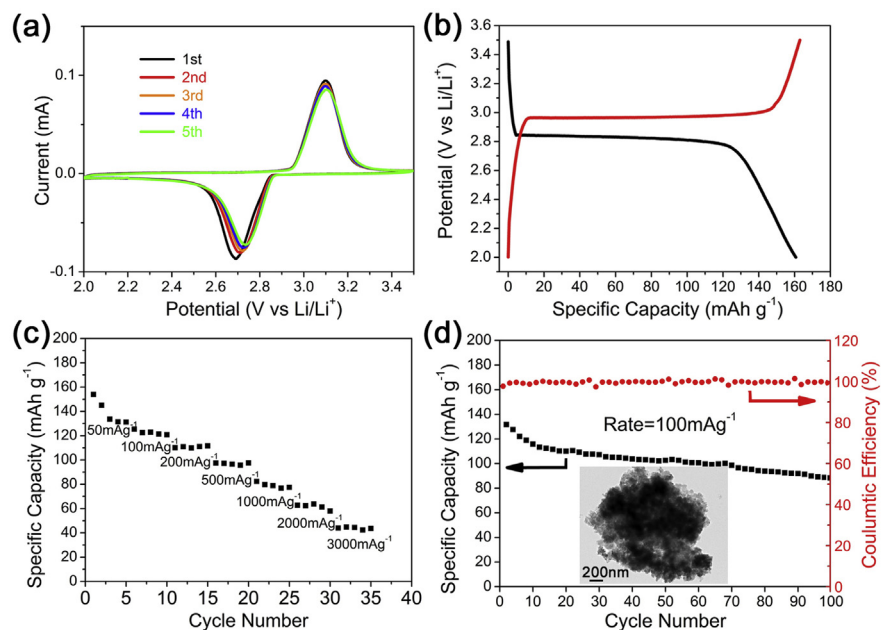


Fig. 5. (a) CV curves for the first five cycles at a scan rate of  $0.1 \text{ mV s}^{-1}$ , (b) charge/discharge curve at a current density of  $50 \text{ mA g}^{-1}$ , (c) the discharge capacities cycled sequentially from 50 to  $3000 \text{ mA g}^{-1}$  for every 5 cycles using a  $50 \text{ mA g}^{-1}$  charge rate, and (d) long-term cycling performance of the as-prepared hierarchical porous  $\text{Li}_4\text{Mn}_5\text{O}_{12}$  nano/micro structure, inset showing the corresponding TEM image after 100 cycles.

#### 4. Conclusions

In summary, we have successfully developed a facile route to synthesize hierarchical porous  $\text{Li}_4\text{Mn}_5\text{O}_{12}$  nano/micro structure using  $\text{MnO}_2$  ultrathin nanoflakes assembled microspheres as self-templates. The resulting unique structure consists of numerous well-crystallized nanoparticles with diameters of  $\sim 20\text{--}30\text{ nm}$ . The adjacent nanoparticles are well-connected with the occurrence of crystal boundary. As predicted, the as-synthesized  $\text{Li}_4\text{Mn}_5\text{O}_{12}$ , when applied as cathodes for LIBs, exhibited a very high specific capacity of  $161\text{ mAh g}^{-1}$  with intriguing rate capability and cycling stability. Such excellent electrochemical performances are attributed to the unique hierarchical porous nano/micro structure. The present findings are very important not only for the easy synthesis of the hierarchical porous  $\text{Li}_4\text{Mn}_5\text{O}_{12}$  nano/micro structure, but also for the development of advanced cathode materials with excellent electrochemical performance.

#### Acknowledgments

This work was supported by the National Natural Science Foundation of China (21206043, 21236003, 21322607), the Research Project of Chinese Ministry of Education (113026A), the

Shanghai Rising-Star Program (13QA1401100), and the Fundamental Research Funds for the Central Universities.

#### References

- [1] P.G. Bruce, B. Scrosati, J.M. Tarascon, *Angew. Chem. Int. Ed.* 47 (2008) 2930.
- [2] S.J. Guo, S.J. Deng, *Chem. Soc. Rev.* 40 (2011) 2644.
- [3] R. Benedek, M.M. Thackray, *J. Phys. Chem. C* 116 (2012) 4050.
- [4] S.H. Lee, Y. Cho, H. Song, K.T. Lee, J. Cho, *Angew. Chem. Int. Ed.* 51 (2012) 8748.
- [5] J.S. Kim, K. Kim, W. Cho, W.H. Shin, R. Kanno, J.W. Choi, *Nano Letters* 12 (2012) 6358.
- [6] M. Hirayama, H. Ido, K. Kim, W. Cho, K. Tamura, J. Mizuki, R. Kanno, *J. Am. Chem. Soc.* 132 (2010) 15268.
- [7] B. Ammundsen, J. Paulsen, *Adv. Mater.* 13 (2001) 943.
- [8] Y.P. Jiang, J. Xie, G.S. Cao, X.B. Zhao, *Electrochim. Acta* 56 (2010) 412.
- [9] Y. Tian, D.R. Chen, X.L. Jiao, Y.Z. Duan, *Chem. Commun.* 20 (2007) 72.
- [10] J.J. Urban, W.S. Yun, Q. Gu, H. Park, *J. Am. Chem. Soc.* 124 (2002) 1186.
- [11] Y.G. Guo, J.S. Hu, L.J. Wan, *Adv. Mater.* 20 (2008) 2878.
- [12] Z.Y. Zeng, X. Huang, Z.Y. Yin, H. Li, Y. Chen, Q. Zhang, J. Ma, F. Boey, H. Zhang, *Adv. Mater.* 24 (2012) 4138.
- [13] J.L. Li, C.B. Cao, X.Y. Xu, Y.Q. Zhu, R.M. Yao, *J. Mater. Chem. A* 1 (2013) 11848.
- [14] L. Shen, C.Z. Yuan, H.J. Luo, X.G. Zhang, K. Xue, Y.Y. Xia, *J. Mater. Chem.* 20 (2010) 6998.
- [15] H. Jiang, T. Sun, C.Z. Li, J. Ma, *J. Mater. Chem.* 22 (2012) 2751.
- [16] M. Manickam, P. Singh, T.B. Issa, S. Thurgate, R.D. Marco, *J. Power Sources* 130 (2004) 254.
- [17] T. Takada, H. Hayakawa, E. Akiba, F. Izumi, B.C. Chakoumakos, *J. Power Sources* 68 (1997) 613.